

# PHYSICAL REVIEW B

## CONDENSED MATTER

THIRD SERIES, VOLUME 39, NUMBER 3

15 JANUARY 1989-II

### Angular distribution of photoelectrons from silver bromide and metallic silver through the Cooper minimum

G. N. Kwawer and T. J. Miller

*Department of Physics, University of Illinois, Urbana, Illinois 61801*

M. G. Mason and Y. Tan

*Research Laboratories, Eastman Kodak Company, Rochester, New York 14650*

F. C. Brown and Y. Ma

*Department of Physics, University of Washington, Seattle, Washington 98195*

(Received 25 April 1988; revised manuscript received 1 September 1988)

Using polarized synchrotron radiation, angle-resolved photoemission data were obtained on randomly oriented polycrystalline AgBr and on thick films of metallic silver. Asymmetry parameters as well as relative cross sections were determined for the valence bands of both systems from 55 eV through the Ag 4*d* Cooper minimum at 140 eV. Comparison of asymmetry parameters with atomic data indicates that the valence bands derived from Ag 4*d* levels in these systems are remarkably atomiclike. In AgBr only the uppermost valence bands show a greatly reduced excursion of the  $\beta$  value through the Cooper minimum.

#### I. INTRODUCTION

It is well known that the angular distribution of electrons photoemitted from randomly oriented atoms or molecules is anisotropic. This is described in early work by Bethe and Salpeter<sup>1</sup> and more recently by Cooper and Zare.<sup>2</sup> There are, for example, a number of published studies which report on investigations of the angular distribution of photoelectrons from both atoms<sup>3</sup> and molecules<sup>4</sup> in the gas phase. The question arises as to how these results are modified in the condensed phase where different initial and final states are involved.

In 1980 Davis *et al.*<sup>5</sup> showed that it was possible to observe photoelectron angular distributions from polycrystalline solids which are at least reminiscent of atomic distributions. Very recently Ardehali and Lindau<sup>6</sup> have compared the angular distributions from a partial monolayer of Ag atoms condensed on a clean silicon surface with the distribution for evaporated silver metal. Here we report results for the valence band of the ionically bonded compound AgBr and compare with new results on silver metal. In the metal the Ag 4*d* levels lie a few volts below the Fermi level, and in AgBr they thoroughly mix with the Br 4*p* levels to form the valence band. Both photoionization cross section and angular anisotropy were observed using synchrotron radiation over a wide range of photon energy from 55 eV through the Ag 4*d* Cooper minimum<sup>7</sup> near 140 eV.

The key quantities of interest in the photoelectron dynamics of atoms and molecules are the angle-integrated partial cross sections and the differential cross sections in angle. In principle, both the integrated and the differential cross sections can be calculated when the

initial- and final-state wave functions are known. Extensive comparison between experiment and theory has been made for atoms and molecules, but so far little has been done for solids.

In the next section we give a brief introduction to the background atomic theory. Later the results for atoms will be compared with results for the condensed phase. The experimental method and details on sample preparation are given in Sec. III. Results are described in Sec. IV, first for thick randomly oriented polycrystalline layers of silver metal, and then for AgBr. Conclusions are given in Sec. V.

#### II. THE ANGULAR DISTRIBUTION PARAMETER: ATOMIC CONSIDERATIONS

Although there are no intrinsic directions in a gas sample, the direction of the incoming photon beam can be used as a reference for the angular distribution of photoelectrons. If the photon beam is plane polarized, one can use the polarization vector as a reference direction. As pointed out by Cooper and Zare,<sup>8</sup> Yang's theorem<sup>9</sup> applies to the angular distribution of photoelectrons from a many-electron atom. For polarized photons, the differential cross section  $d\sigma/d\Omega$  is given by

$$\frac{d\sigma(\gamma, h\nu)}{d\Omega} = \frac{\sigma_{nl}(h\nu)}{4\pi} \left[ 1 + \frac{\beta(h\nu)}{2} (3 \cos^2 \gamma - 1) \right], \quad (1)$$

where  $\gamma$  is the angle between the polarization vector and the outgoing photoelectron and  $\sigma_{nl}$  is the total photoionization cross section for the *nl* subshell. The angular distribution of photoelectrons is determined in large part by the asymmetry parameter  $\beta(h\nu)$ , which is a function of

photon energy. This asymmetry parameter ranges between 2 and  $-1$  with a value  $\beta=0$  corresponding to an isotropic pattern of emission. Excitation from an atomic  $s$  to a  $p$  level gives rise to an angular distribution corresponding to  $\beta=2$  and a distribution proportional to  $\cos^2(\gamma)$ . When  $\beta=-1$  the angular distribution is proportional to  $\sin^2(\gamma)$ .

$$\beta = \frac{l(l+1)\sigma_{l-1}^2 + (l+1)(l+2)\sigma_{l+1}^2 - 6l(l+1)\sigma_{l+1}\sigma_{l-1}\cos(\delta_{l-1} - \delta_{l+1})}{(2l+1)[l\sigma_{l-1}^2 + (l+1)\sigma_{l+1}^2]}, \quad (2)$$

where we have omitted an incorrect factor of  $\frac{1}{3}$  given in an earlier report.<sup>2</sup>

Equation (2) shows that  $\beta$  is very dependent on photoionization cross sections  $\sigma_{l\pm 1}$  and their variation with energy; however, the phase-shift term also determines the exact behavior of the asymmetry parameter. In photon-energy regions where the cross sections are finite and do not vary much with energy,  $\beta$  is most sensitive to the difference in phase shifts between the  $l+1$  and  $l-1$  outgoing waves. For those regions where the cross sections vary rapidly with energy, the asymmetry parameter is primarily controlled by the cross sections. At a Cooper minimum (for example, in the Ag  $4d$  minimum) the cross section for the  $l$  to  $l+1$  channel becomes zero. All terms in Eq. (2) containing the  $l$  to  $l+1$  cross section become zero, and the asymmetry parameter reduces to the value  $\beta=0.6$ . This result is independent of the actual value of the  $l-1$  cross section. Consequently, using data on  $\beta$  as well as  $\sigma$ , one can better pinpoint the location of the Cooper minimum.

Carlson *et al.*<sup>4</sup> have compared experimental asymmetry-parameter data for free atoms with data for the same atoms in molecules. Differences are found which they ascribe, in general, to differences in both initial and final states. Clearly, in the molecule the initial state can be altered by the chemical bonding.

In the case of a randomly oriented polycrystalline solid we expect that the atomic behavior of both  $\sigma$  and  $\beta$  will be observable, although perhaps different in detail compared to atoms. Photoemission from core levels should be closely atomlike. Certainly, the calculated photoionization cross sections<sup>10</sup> for various atoms are an excellent guide to the observed energy dependence for core-level photoemission from solid surfaces. Even valence-band emission is known to reflect the theoretical atomic cross sections. In this paper we will compare valence-band asymmetry parameters for two very different condensed systems and look for contrast to the atomic case.

### III. EXPERIMENTAL DETAILS

Sample preparation and sample geometry were both important aspects of the experiment. Let us first consider sample preparation, which was done *in situ* in a small evaporation chamber adjacent to the angle-resolved photoemission chamber on the University of Illinois beamline at the Synchrotron Radiation Center, Stoughton, Wisconsin. The photoemission experiments were carried out in ultrahigh vacuum using radiation from the Alad-

According to well-known selection rules, an atomic electron with orbital angular momentum  $l$  can be excited by light to a final state with momentum  $l+1$  or  $l-1$ . The asymmetry parameter  $\beta$  can be evaluated in terms of the photoionization cross sections  $\sigma_{nl}$  and phase shifts  $\delta_{l\pm 1}$ .<sup>8</sup> For transitions from an initial state with angular momentum  $l$  to  $l+1$  and  $l-1$  final states, the result is

din storage ring monochromated by an extended range grasshopper monochromator.<sup>11</sup>

Glass disks, 1 cm in diameter overcoated with a thick layer of gold for electrical contact to discharge the sample, were placed in the evaporation chamber and pumped to the high- $10^{-9}$ - or low- $10^{-8}$ -Torr range. A thick layer of silver ( $\approx 1000$  nm) was then evaporated onto the gold surface. Upon completion of the evaporation the sample was transferred through an interlock into the main photoemission chamber where a vacuum better than  $4 \times 10^{-10}$  Torr could be maintained. The silver sample was then argon-ion-etched ( $4 \times 10^{-5}$  Torr, 0.5 kV, 35 mA) for 40 min. This procedure was necessary in order to produce a clean valence-band energy-distribution curve and to further randomize the polycrystalline silver surface. Cross-section and angular-anisotropy experiments on the metallic silver were then carried out in the main chamber.

After photoemission studies of the silver surface, the substrate was moved through the interlock into the evaporation chamber in order to prepare the AgBr sample. The AgBr was evaporated from a platinum-filament source onto the silver surface at 2 Å/s. A thickness of about 400 Å was achieved in order to minimize charging during photoemission runs on the insulating ionic crystal cooled to low temperature. The sample was transferred into the main chamber where it was held on a precision manipulator where it could be cooled to 77 K. The photoemission studies of AgBr were carried out at low temperature in order to minimize photolysis. Care was taken to avoid condensation of contaminants onto the cold sample surface by keeping the vacuum in the main chamber better than  $3 \times 10^{-10}$  Torr.

The angle-resolved photoemission experiments to determine  $\beta$  were carried out using two different geometries. For purposes of discussion let us assume that the incoming radiation is 100% plane polarized in the horizontal plane. Later a correction will be made to account for partial polarization. In the first series of tests electron emission in the horizontal plane was observed at angles of  $\gamma_1=0^\circ$  and  $\gamma_2=54.7^\circ$  measured with respect to the polarization vector of the light. At these angles especially simple values of  $d\sigma/d\Omega$  result. For example, at  $\gamma=0$  Eq. (1) reduces to

$$\frac{d\sigma(0, h\nu)}{d\Omega} = \frac{\sigma_{nl}(h\nu)}{4\pi} (1 + \beta). \quad (3)$$

At  $\gamma=54.7^\circ$ , the so-called magic angle, Eq. (1) becomes

$$\frac{d\sigma(54.7, h\nu)}{d\Omega} = \frac{\sigma_{ni}(h\nu)}{4\pi}, \quad (4)$$

which gives the cross section and its variation with energy. At a given angle  $\gamma$  and photon energy  $h\nu$  the observed electron-counting rate  $N$  is proportional<sup>12</sup> to  $d\sigma/d\Omega$ , to the analyzer transmission  $T(E_k)$  as a function of electron kinetic energy  $E_k$ , to the photoelectron escape depth  $\lambda(E_k)$ , to the relative photon flux arriving at the sample,  $\Phi(h\nu)$ , and to a function  $F$  which depends on reflection and refraction at the surface of the sample, i.e.,

$$N(\gamma, h\nu) \propto \frac{d\sigma(\gamma, h\nu)}{d\Omega} T(E_k) \lambda(E_k) \Phi(h\nu) F. \quad (5)$$

Now if the geometry of the experiment can be arranged so that, for the two different angles  $\gamma$ , all factors in Eq. (5) remain constant except the differential cross sections, then  $\beta$  can be evaluated from the ratio of counting rates  $R = N(0, h\nu)/N(54.7, h\nu)$ . Using Eqs. (3) and (4), this gives

$$R = 1 + \beta. \quad (6)$$

Southworth *et al.*<sup>1</sup> and Hecht and Lindau<sup>13</sup> have discussed the difficulties in accurately determining  $\beta$  using the geometry described above and a more general geometry. Hecht and Lindau point out, for example, the desirability of keeping the electron-escape depth the same for the two angles of  $\gamma$ . In the present experiment this was accomplished by moving the small hemispherical electron analyzer<sup>14</sup> in the horizontal plane to equal angles  $\gamma_1 = 0^\circ$  and  $\gamma_2 = 54.7^\circ$  on either side of the sample normal. For this purpose the sample was set in a fixed position by rotating about an axis perpendicular to the horizontal plane. The incoming photon beam was thus inclined to the sample surface, which was fine at the higher photon energies where the index of refraction was close to 1.00. At the lower photon energies it was necessary to make a correction for refraction at the interface using the known indices of refraction for Ag metal<sup>15</sup> and AgBr.<sup>16</sup> Reasonable results for both materials were obtained in this way, but a more accurate method which did not require a correction for the refracted beam direction within the sample was therefore developed. This new method is described in the next paragraph.

We now define the ratio of count rates  $R = N(\gamma_1, h\nu)/N(\gamma_2, h\nu)$  at two angles of electron collection  $\gamma_1$  and  $\gamma_2$  measured with respect to the polarization vector. Taking the ratio of counting rates using Eq. (1) and solving for  $\beta$ , it is not hard to show that the asymmetry parameter is given by

$$\beta = \frac{2(R-1)}{(3\cos^2\gamma_1-1) - R(3\cos^2\gamma_2-1)}, \quad (7)$$

all other factors in Eq. (5) remaining constant. In this second method of data acquisition the sample was placed so that the incoming photon beam was normal to its surface as indicated in Fig. 1. The electron analyzer could then be positioned anywhere on the cone of rays shown in the figure, and it would intercept electrons with the same

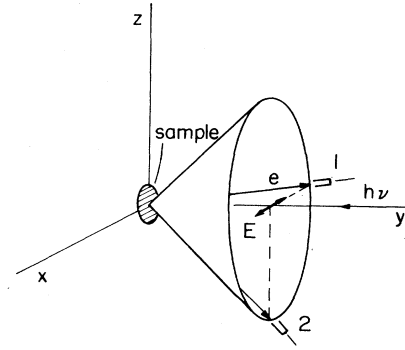


FIG. 1. Sample geometry showing the two electron-analyzer positions, (1)  $33^\circ$  and (2)  $90^\circ$  used for determining the asymmetry parameter. The electron analyzer could also be positioned at  $\gamma = 54.7^\circ$  in the horizontal plane for cross-section measurements. The synchrotron radiation is plane polarized in the horizontal plane and incident normal to the sample surface as shown.

angle of escape, referred to the sample normal. The electron-escape path length within the sample would thus be the same for different angles. Accordingly, a simple ratio of counting rates could be obtained in order to determine  $\beta$  from Eq. (7). For good results the cone angle was chosen to be  $33^\circ$ , which corresponds to  $\gamma_1 = 33^\circ$ , position 1 in Fig. 1. Position 2, out of the horizontal plane, was then chosen to correspond to  $\gamma_2 = 90^\circ$ . At these angles Eq. (7) reduces to

$$\beta = \frac{2(R-1)}{1.11+R}. \quad (8)$$

In practice, Eq. (8) had to be modified because the synchrotron radiation incident upon the sample was not 100% plane polarized. In fact, the polarization of the radiation incident upon the monochromator can be accurately calculated. It turns out to be close to  $P = (I_{\parallel} - I_{\perp}) / (I_{\parallel} + I_{\perp}) = 0.7$  throughout the range of photon energies utilized. Since reflections in the monochromator were all at low grazing angles ( $1^\circ$  and  $2^\circ$ ), we expect the incoming polarization to be fairly well maintained. Rewriting  $P$  as  $P = (\alpha - 1) / (\alpha + 1)$ , where  $\alpha = I_{\parallel} / I_{\perp}$ , a polarization  $P$  of 70% corresponds to  $\alpha = 5.67$ . If one now repeats the analysis leading to Eq. (8) by adding separate contributions to the counting rate at each angle from the two intensities of polarization  $I_{\parallel}$  and  $I_{\perp}$ , the result is an expression for  $\beta$  containing corrections  $\epsilon = 1/\alpha$ . For  $\gamma_1 = 33^\circ$  in the horizontal plane and  $\gamma_2 = 90^\circ$  with the analyzer in the vertical plane, the result is

$$\beta = \frac{2[R(1+\epsilon) - (1+\epsilon)]}{1.11 - \epsilon + R(1-\epsilon)}. \quad (9)$$

Equation (9) was used to calculate the corrected values of  $\beta$  presented and discussed in the next section.

Relative cross-section measurements on Ag metal were obtained by setting the hemispherical analyzer to  $\gamma = 54.7^\circ$  in the horizontal plane. Energy-distribution curves could be obtained in this way with an energy reso-

lution of about 0.3 eV, determined by both the monochromator bandwidth and the analyzer resolution. During all experiments the photon flux was monitored by recording the total electron yield from an 80% transmitting gold screen placed at an appropriate place in the monochromated synchrotron-radiation beam. All distributions and scans were recorded using an LSI-1123 computer and the data-collection system described in Ref. 14.

#### IV. RESULTS AND DISCUSSION

In order to test our methods for determining  $\beta$ , the Ag 4s core level (binding energy about 97 eV) in the metal was investigated. For a moderately deep core like this we expect atomic behavior and excitation to a  $p$ -like final state. The asymmetry parameter should be quite close to  $\beta=2$ . Experimentally, a value  $\beta=1.93\pm 0.2$  was obtained, which is reasonably close to the expected value.

Further experiments which were carried out on the metallic silver films included the valence-band energy-distribution curves, relative cross section as a function of energy, and asymmetry parameter for the  $d$ -like contributions to the valence band. Figure 2 shows the valence-band energy-distribution curves at  $\gamma=54.7^\circ$  for photon energies below and extending through the Cooper minimum at 140 eV. Note that each of these four scans has a different counting-rate scale. The electron analyzer was run in such a way that its transmission was approxi-

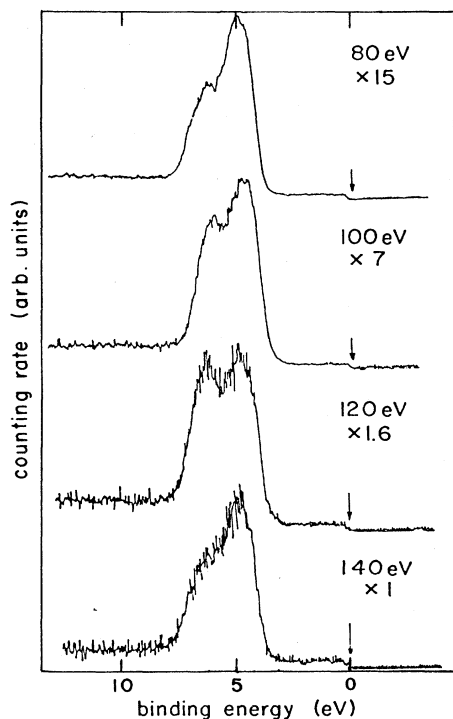


FIG. 2. Energy-distribution curves for the valence band of Ag metal below and through the Cooper minimum at 140 eV. Note the difference in counting-rate scales for each case—and also the fact that the photon flux from the monochromator is about 4 times greater at 140 eV than at 80 eV. Arrows indicate the Fermi level.

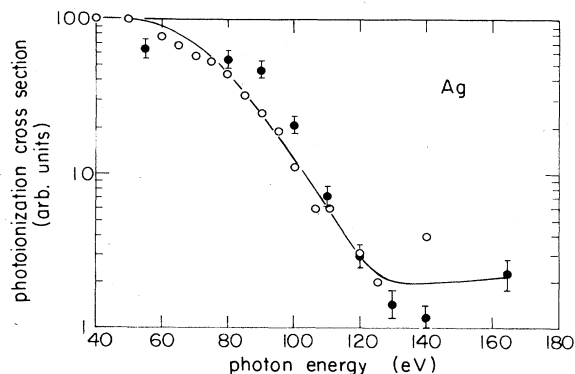


FIG. 3. Measured photoionization cross section on a logarithmic scale for metallic silver shown by solid points with error bars. The open circles are the values for atoms measured by Krause *et al.*, Ref. 3, whereas the results for theory are indicated by the solid line.

mately constant over the energy range covered. Notice that there is considerable reduction in observed photoyield in going from 50 to 140 eV, especially if one takes into account the fact that the incident photon flux from the monochromator increases substantially over this range.

At low energy a slowly rising background due to secondary electrons can be seen in Fig. 2. These data could be analyzed using an interactive data program which allowed us to subtract background and to determine the area between specified energies encompassing the  $d$  bands. This area was then divided by the recorded mesh current corrected by the known electron yield of gold.<sup>17</sup> In this way the data could be corrected for changes in incident-photon flux, yielding a set of numbers proportional to the partial photoionization cross section for the Ag 4d band. This measured relative cross section is plotted on a logarithmic scale in Fig. 3 as solid data points with error bars. Our experimental data is least-squares-fitted to the theoretical cross section for silver<sup>3</sup> shown by a solid curve. The open circles are the data points for silver atoms measured by Krause *et al.*<sup>3</sup>

Notice that the experimental points for our evaporated and ion-etched silver sample cover almost two decades through the Cooper minimum. This is more like the data for isolated Ag atoms in the work of Ardehali and Lindau.<sup>6</sup> The Cooper minimum appears to be shifted slightly to higher energy, as in Davis's data for silver,<sup>5</sup> which, however, has a more shallow minimum than our data.

Figure 4 shows photoemission data taken at  $h\nu=100$  eV, and it illustrates how the asymmetry parameter  $\beta$  was obtained for the  $d$ -derived bands of metallic silver. Two curves are shown after background subtraction, one at  $\gamma_1=33^\circ$  and the other at  $\gamma_2=90^\circ$ . Both curves have been normalized to the same beam current. Integration under the main bands from 86 to 90.5 eV allows one to compute the ratio of areas for this band. This ratio turns out to be  $R = \frac{2651}{931} = 2.86$ , which yields  $\beta=1.36$  using Eq. (9).

In Fig. 5 we plot as solid points with error bars the experimental values of  $\beta$  as a function of photon energy. Also shown as a dotted line are the data of Krause *et al.*<sup>3</sup>

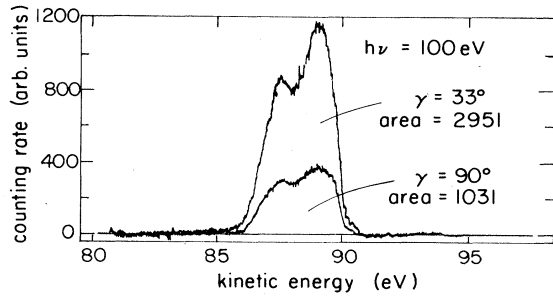


FIG. 4. Energy-distribution curves for a silver film taken at a photon energy of 100 eV and at two different angles of collection  $\gamma$ . The secondary-electron background has been subtracted from these data, and the two curves have been normalized to the same storage-ring beam current.

on silver atoms. Notice that the data on the metallic silver film are very much like the data on atoms. Of interest is the fact that the energy for  $\beta=0.6$  is similar in both cases, suggesting that the Cooper minimum is not greatly shifted in the condensed phase.

Let us now turn to measurements of the asymmetry parameter for the compound AgBr. Energy-distribution curves of the valence band of randomly oriented polycrystalline AgBr are shown in Fig. 6. The top of the valence band is indicated by an arrow in each case. There are four main features centered at 1.5, 3.0, 3.8, and 4.4 eV below the top of the valence band. Separation of these various band components was carried out by fitting the data with Gaussian distributions, as well as by integrating to determine the area between selected energies. Very similar results were obtained using these two different methods.

The angle-integrated photoemission experiments<sup>18-20</sup> on the silver halides as well as the early band calculations of Bassani and co-workers<sup>21</sup> indicate, at least in a qualitative fashion, how the valence bands of these compounds are composed of different amounts of Ag 4*d* and Br 4*p*

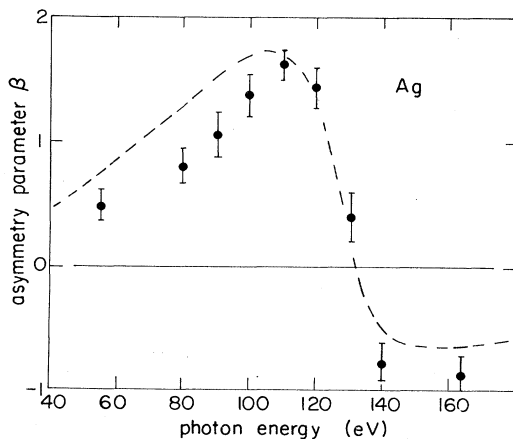


FIG. 5. Measured asymmetry parameters for silver metal (solid points with error bars) compared with  $\beta$  values for Ag atoms (dashed line) obtained by Krause *et al.* (Ref. 3).

character. More recently, data taken at low temperature<sup>22</sup> permits one to extract the Ag 4*d* and Br 4*p* density from the total density of states. Figure 7 shows these separate contributions. There is strong mixing throughout the bands, but the lower-energy regions (higher binding energy) are predominantly *d*-like, whereas the upper band is largely Br 4*p*.

Asymmetry parameters for the valence bands of AgBr are plotted in Fig. 8. Here we have chosen to combine the areas of the more deeply bound "d bands" and to plot separately the uppermost *p/d* band. Notice that the "d bands" behave very much like the *d* bands of Ag metal, especially as to the position of the Cooper minimum ( $\beta=0.6$ ). The uppermost band is a real admixture of *p*- and *d*-derived states, and it can be seen that the value  $\beta=0.6$  is shifted to slightly higher energy. Likewise, the range of the  $\beta$  parameter is considerably reduced for this uppermost *p/d* band.

## V. CONCLUSIONS

There is now a growing accumulation of experimental evidence that Cooper-minimum phenomena, including observation of the asymmetry parameter, can be studied in the condensed phase as well as in gases. For this purpose we have found it important to work with randomly

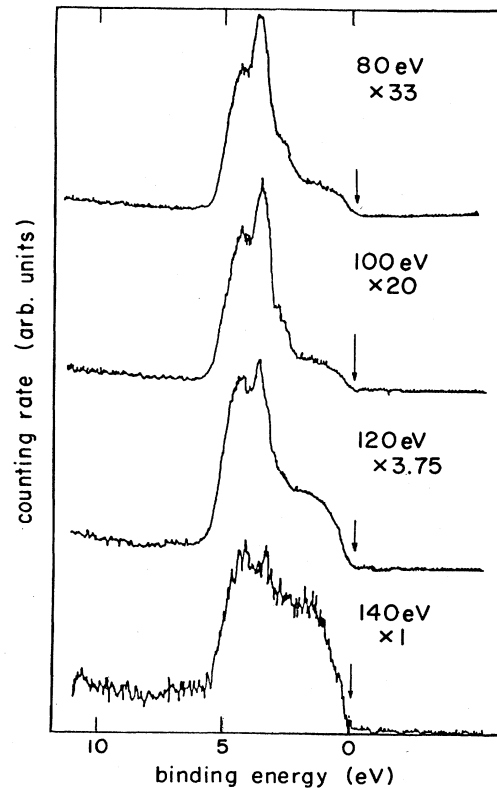


FIG. 6. Energy-distribution curves for the valence band of randomly oriented polycrystalline AgBr below and through the Cooper minimum at 140 eV. Similar comments on the counting-rate scales apply as in Fig. 2. Data taken with the AgBr sample at 77 K.

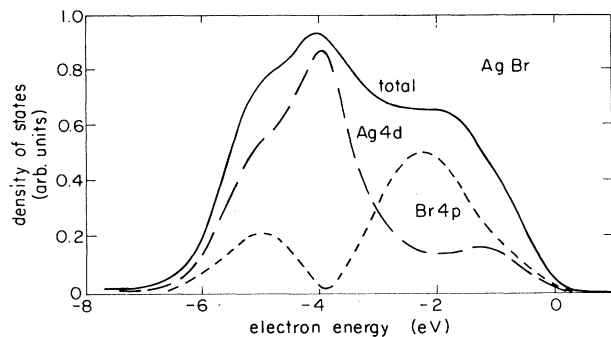


FIG. 7. Estimated valence-band density of states for AgBr showing the separated Ag 4*d*- and Br 4*p*-derived contributions. From Mason *et al.* (Ref. 20).

oriented polycrystalline samples. In this paper, after describing the experimental method, we have presented angular-anisotropy data for the valence band of the compound AgBr through the Ag 4*d* Cooper minimum from 55 to 165 eV. Similar data are also presented for metallic silver.

For the 4*d*-derived valence bands of silver metal, the results on the energy dependence of both partial and differential cross sections are remarkably atomiclike. Only the depth of the excursion in asymmetry parameter through the Cooper minimum is slightly reduced in the solid. In fact, the results presented here on the metal are somewhat more atomiclike than reported by other authors.<sup>5,6</sup> The observed cross section for the *d*-derived bands covers almost 2 orders of magnitude through the Cooper minimum. Likewise, the excursion in asymmetry parameter through the Cooper minimum is larger than previously reported for evaporated silver. We find that the dispersionlike behavior of the asymmetry parameter is a good way to locate the Cooper minimum, even in the condensed phase.

Our method gave a value of  $\beta$  close to 2.0 for the Ag 4*s* core, which gives one confidence in the experimental method. The difference in our measured  $\beta$  value from previously reported work on the metal may be due to differences in samples. In our case, special care was taken to clean and randomize the surface by argon-ion bombardment. This procedure resulted in valence-band energy-distribution curves of the highest quality, which apparently was important in obtaining the cross-section and asymmetry-parameter data. We also found that it was important to have the photon beam perpendicular to the sample surface; otherwise in oblique geometry rather large corrections for refraction at the interface had to be made, especially in the range of photon energy between 60 and 100 eV.

The experimental results on asymmetry parameter for AgBr can likewise be readily compared with the atomic behavior of silver. The excursions in  $\beta$  value for the deeper *d*-derived valence bands are only slightly reduced from atomic values. The overall behavior of the valence-band asymmetry in AgBr can best be understood in terms of the well-known valence-band structure for the compound, which is a mixture of *d*- and *p*-derived band densi-

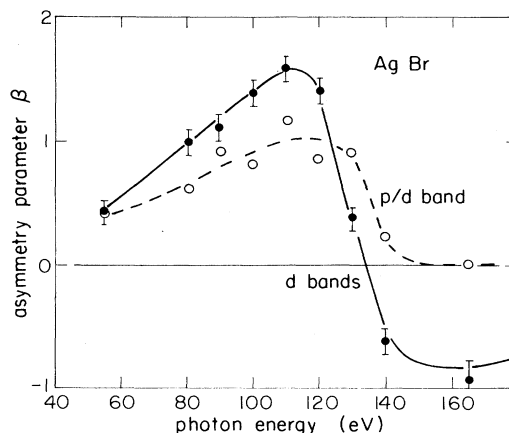


FIG. 8. Asymmetry parameter as a function of photon energy for randomly oriented polycrystalline AgBr. Data for the three most deeply bound components (mainly Ag 4*d* bands) are shown by solid points and the solid line, whereas the least-bound *p*-*d* component band is shown by open circles and a dotted curve.

ty. Whereas the asymmetry of the deeper *d*-derived valence bands are remarkably atomiclike, the variation in  $\beta$  value through the Cooper minimum for the uppermost *p*-*d* valence band of AgBr is much reduced compared to the atomic case. It is also slightly shifted to higher energy. To a great extent these results can be understood in terms of substantial admixture of *p*-like wave function into the initial state. The admixture is important throughout the valence band of the ionic crystal, but most important for the uppermost band, which is derived primarily from Br *p* states.

A comparison here of measured  $\beta$  values for solids with those obtained or calculated for atoms leads to conclusions a lot like those stated by Carlson and co-workers,<sup>4</sup> who compared atoms and molecules. The behavior of the  $\beta$  value dramatically attests to Cooper-minimum phenomena even in the solid. In fact, the excursion and shifted position of the minimum is probably best determined from data on the  $\beta$  value. One can speculate on the effects of bonding in the solid as it affects both initial and final states. Clearly, the silver 4*d*-derived bands in the ionic crystal AgBr are highly atomic in nature. It would be most useful, however, to have a calculation of the matrix elements important in the  $\beta$  value for the solid. For this purpose it would be necessary to have realistic wave functions.

#### ACKNOWLEDGMENTS

The authors would like to acknowledge support from the National Science Foundation under Grant No. DMR-88-96157. Additional support from the Eastman Kodak Company (Rochester, NY) is also much appreciated. The Synchrotron Radiation Center (Stoughton, WI) is supported by the National Science Foundation under Grant No. DMR-86-01349.

- <sup>1</sup>H. Bethe and E. Salpeter, *Quantum Mechanics of One and Two Electron Atoms* (Academic, New York, 1957).
- <sup>2</sup>J. W. Cooper and R. N. Zare, *J. Chem. Phys.* **48**, 942 (1968).
- <sup>3</sup>M. O. Krause, W. Swensson, T. A. Carlson, G. Leroi, D. E. Ederer, D. Holland, and A. C. Parr, *J. Phys. B* **18**, 4069 (1985).
- <sup>4</sup>T. A. Carlson, M. O. Krause, W. A. Svensson, P. Gerard, F. A. Grimm, T. A. Whitley, and B. P. Pullen, *Z. Phys. D* **2**, 309 (1986).
- <sup>5</sup>R. F. Davis, S. D. Kevan, B. C. Lu, J. G. Tobin, and D. A. Shirley, *Chem. Phys. Lett.* **71**, 448 (1980).
- <sup>6</sup>M. Ardehali and I. Lindau, *J. Electron Spectrosc. Relat. Phenom.* **46**, 215 (1988).
- <sup>7</sup>J. W. Cooper, *Phys. Rev.* **128**, 681 (1962).
- <sup>8</sup>J. W. Cooper and R. N. Zare, in *Lectures in Theoretical Physics*, edited by S. G. Geltman, K. Mahanthappa, and W. Brittin (Gordon and Breach, New York, 1969), Vol. II C, p. 317.
- <sup>9</sup>C. N. Yang, *Phys. Rev.* **74**, 764 (1948).
- <sup>10</sup>J. Yeh and I. Lindau, *At. Data Nucl. Data Tables* **31**, 211 (1985).
- <sup>11</sup>S. L. Hulbert, J. P. Stott, and F. C. Brown, *Nucl. Instrum. Meth.* **208**, 43 (1983).
- <sup>12</sup>S. Southworth, C. M. Truesdale, P. H. Kobrin, D. W. Lindle, W. D. Brewer, and D. A. Shirley, *J. Chem. Phys.* **76**, 143 (1982).
- <sup>13</sup>M. H. Hecht and I. Lindau, *J. Electron Spectrosc. Relat. Phenom.* **35**, 211 (1985).
- <sup>14</sup>T. J. Miller, Ph.D. thesis, University of Illinois–Urbana Champaign, 1986 (unpublished).
- <sup>15</sup>H. J. Hagemann, W. Gudat, and C. Kunz, *J. Opt. Soc. Am.* **65**, 742 (1975).
- <sup>16</sup>N. Carrera and F. C. Brown, *Phys. Rev. B* **4**, 3651 (1971).
- <sup>17</sup>B. Henke, P. Lee, T. J. Tanaka, R. L. Skimabukuro, and B. K. Fujikawa, *At. Data Nucl. Data Tables* **27**, 1 (1982).
- <sup>18</sup>J. Tejada, N. J. Shevchik, W. Braun, A. Goldmann, and M. Cardona, *Phys. Rev. B* **12**, 1557 (1975).
- <sup>19</sup>R. S. Bauer and W. E. Spicer, *Phys. Rev. B* **14**, 4539 (1976); *Phys. Rev. Lett.* **25**, 1283 (1970).
- <sup>20</sup>M. G. Mason, *Phys. Rev. B* **11**, 5094 (1975).
- <sup>21</sup>F. Bassani, R. S. Knox, and W. B. Fowler, *Phys. Rev.* **137**, A1217 (1965).
- <sup>22</sup>M. G. Mason, G. N. Kwawer, F. C. Brown, Y. Tan, and T. J. Miller (unpublished).